JPET Fast Forward. Published on December 12, 2006 as DOI: 10.1124/jpet.106.114884

Comparison of Lorazepam Occupancy of Rat Brain $GABA_A$ Receptors Measured Using In Vivo [^{3}H]Flumazenil Binding and [^{11}C]Flumazenil microPET

John R. Atack, Paul Scott-Stevens, John Beech, Tim D. Fryer, Jessica L. Hughes, Marcel C. Cleij, Jean-Claude Baron, John C. Clark, Richard J. Hargreaves and Franklin I. Aigbirhio

Merck Sharp & Dohme Research Laboratories, Neuroscience Research Centre, Terlings Park, Eastwick Road, Harlow, Essex CM20 2QR, United Kingdom (JRA, PSS)

Department of Anaesthesia, Addenbrookes Hospital, Cambridge, United Kingdom (JB)

Wolfson Brain Imaging Centre, Addenbrookes Hospital, Cambridge, United Kingdom (TDF, MCC, JCB, JCC, FIA)

Department of Clinical Neurosciences, Addenbrookes Hospital, Cambridge, United Kingdom (JLH)

Imaging Research and Pharmacology, Merck Research Laboratories, West Point, PA, USA (RJH)

Running title: Comparison of rat brain lorazepam occupancy methodologies

Address correspondence, proofs and reprint requests to Dr. John R. Atack at his present address: Neuroscience, Johnson & Johnson Pharmaceutical Research and Development, 3210 Merryfield Row, La Jolla, CA 92121, USA.

Tel: 858-320-3498

Fax: 858-450-2040

E-mail: JAtack@prdus.jnj.com

Number of text pages:	27
Number of tables:	2
Number of figures:	8
Number of references:	40
Words in abstract:	243
Words in Introduction:	525
Words in Discussion:	1,234

Abbreviations: PET, positron emission tomography; flumazenil, 8-fluoro 5,6-dihydro-5-methyl-6-oxo-4*H*-imidazo[1,5-*a*][1,4]benzodiazepine-3-carboxylic acid ethyl ester; Lorazepam, 7-Chloro-5-(2-chlorophenyl)-1,3-dihydro-3-hydroxy-2*H*-1,4-benzodiazepin-2-one

ABSTRACT

The occupancy by lorazepam of the benzodiazepine binding site of rat brain $GABA_A$ receptors was compared when measured using either in vivo binding of [^{3}H]flumazenil in terminal studies or [^{11}C]flumazenil binding in anaesthetised animals assessed using a small animal positron emission tomography scanner (microPET). In addition, as a bridging study, lorazepam occupancy was measured using [^{3}H]flumazenil in vivo binding in rats anaesthetized and dosed under microPET conditions. Plasma lorazepam concentrations were also determined and for each occupancy method, the concentration required to produce 50% occupancy (EC_{50}) was calculated, since this parameter is independent of the route of lorazepam administration. For the in vivo binding assay, lorazepam was dosed orally (0.1-10 mg/kg) whereas for the microPET study lorazepam was given via the i.v. route as a low dose (0.75 mg/kg bolus) and then a high dose (0.5 mg/kg bolus then 0.2 mg/ml infusion). The lorazepam plasma EC_{50} in the [^{11}C]flumazenil microPET study was 96 ng/mL (95% confidence intervals (95% CI) = 74-124 ng/mL) which was very similar to the [^{3}H]flumazenil microPET simulation study (94 ng/mL; 95% CI = 63-139 ng/mL) which in turn was comparable to the [^{3}H]flumazenil in vivo binding study (134 ng/mL; 95% CI = 119-151 ng/mL). These data clearly show that despite the differences in dosing (i.v. in anaesthetized versus orally in conscious rats) and detection (in vivo dynamic PET images versus ex vivo measurements in filtered and washed brain homogenates), [^{11}C]flumazenil microPET produces results similar to [^{3}H]flumazenil in vivo binding.

Introduction

The pharmacological effect of any drug is a function of its intrinsic efficacy and the extent to which it occupies the target, whether that target is an enzyme, transporter or receptor. The extent to which a drug occupies its target is related to its affinity for the target as well as its concentration. In peripheral tissues for which there is a negligible plasma:tissue barrier, drug concentrations in the plasma can be used as a surrogate of those in the target tissue. However, this is not the case for the CNS since the blood:brain barrier restricts penetration of drug into the CNS. Consequently, plasma drug concentrations may be misleading when interpreting the pharmacological effects of CNS drugs and therefore it is necessary to measure the extent to which they occupy the protein of interest. An additional attraction of measuring occupancy is that it is a parameter that can be quantified not only in preclinical species but also in man, provided that there is available a radioligand suitable for human positron emission tomography (PET) use (Wang and Maurer, 2005).

The methods generally used to measure occupancy in the brain of preclinical species and in man are very different, raising the possibility that methodological differences may be a factor in the translation of occupancy measurements from preclinical species into man. Hence, in preclinical species, occupancy is generally assessed by measuring the extent to which predosing an animal with test compound inhibits either the degree of binding of a radioligand administered to the live animal (in vivo binding; e.g., Atack et al., 1999) or the binding of radioligand incubated with brain tissue after the animal is killed (ex vivo binding; e.g., Duffy et al., 2002), with, for methodological reasons, in vivo binding being preferred to ex vivo binding (Li et al., 2006). With in vivo binding, the quantitation of radioactivity in the brain necessitates removal of the brain, homogenization and filtration and washing, the latter of which removes free ligand and low-affinity non-specific binding, followed by liquid scintillation counting. On the other

hand, in PET studies brain radioactivity is detected in live subjects and comprises radioactivity in the specific and non-specific binding, free radioligand and blood compartments.

With the availability of small animal scanners, such as the microPET (Tai et al., 2001; Yang et al., 2004; Cheery and Chatiioannou, 2005), it is now possible to perform PET in rodents. The purpose of the present study was to measure occupancy using microPET techniques and compare these data to those obtained by more traditional in vivo binding methods. More specifically, lorazepam (7-Chloro-5-(2-chlorophenyl)-1,3-dihydro-3-hydroxy-2*H*-1,4-benzodiazepin-2-one) occupancy of the benzodiazepine binding site of rat brain $GABA_A$ receptors was measured using the inhibition of the in vivo binding of radiolabeled flumazenil (8-fluoro 5,6-dihydro-5-methyl-6-oxo-4*H*-imidazo[1,5-*a*][1,4]benzodiazepine-3-carboxylic acid ethyl ester) in terminal homogenization and filtration or in vivo microPET assays using [^{3}H]flumazenil or [^{11}C]flumazenil, respectively. In addition, a bridging study was performed in which lorazepam occupancy was measured under simulated microPET conditions but using [^{3}H]flumazenil in vivo binding methods. Since these methods employed different dosing routes (oral for in vivo [^{3}H]flumazenil binding and i.v. for [^{11}C]microPET) plasma-occupancy relationships were determined since these are independent of drug dose route and the plasma lorazepam concentration required to give 50% occupancy (EC_{50}) was calculated.

Materials and Methods

All aspects of animal care and use complied with the UK Animals (Scientific Procedures) Act 1986 and its associated guidelines.

Drugs

Lorazepam was obtained from Sigma Aldrich whilst bretazenil was synthesised at Merck Research

Laboratories (Harlow, UK). [^{3}H]Flumazenil ([^{3}H]Ro 15-1788; 87 Ci/mmol) was obtained from PerkinElmer LAS (Boston, MA).

[^{3}H]Flumazenil in vivo binding

Male CD (Sprague-Dawley-derived) rats (250-300g, Charles River UK Ltd, Ramsgate, Kent, UK; n=5-10/group) received either vehicle (0.5% methyl cellulose p.o. with a dosing volume of 5 mL/kg), lorazepam (0.1, 0.3, 1, 3, 5 or 10 mg/kg) or, to define the level of non-specific binding, bretazenil (5 mg/kg i.p. in 100% polyethylene glycol 300). This dose of bretazenil was chosen since it gives 100% occupancy of the benzodiazepine binding site of rat brain $GABA_A$ receptors (Atack et al., 2006). Twenty-seven minutes later, animals received an i.v. tail vein injection of [^{3}H]flumazenil (diluted 1:150 with saline and dosed at 1 μL/g; equivalent to a dose of 2 μCi [^{3}H]flumazenil/300 g rat) and after a further 3 min. were culled by decapitation. Trunk blood was collected into lithium-heparin tubes, centrifuged and plasma retained for subsequent analysis for drug concentrations (see below). Brains were removed, and rapidly homogenised in 10 volumes ice-cold buffer (50 mM potassium phosphate, pH 7.4 containing 100 mM KCl) and 300 μL aliquots filtered and washed with 10 mL buffer over Whatman GF/B filters. The filters were then placed in scintillation vials, scintillation fluid was added and radioactivity counted on a Beckman LS6500 scintillation counter. The radioactivity in bretazenil-treated animals (c. 100 dpm) was subtracted from each of the other groups to give specific binding which was in the region of 2000 dpm in vehicle-treated rats. In lorazepam-treated animals, the extent by which radioactivity was reduced relative to the vehicle group represented the extent to which lorazepam occupied the benzodiazepine binding site of rat brain $GABA_A$ receptors.

Measurement of plasma lorazepam concentrations

Aliquots of plasma (50μL) were prepared for analysis by protein precipitation using 3 volumes of acetonitrile containing internal standard, diazepam. Following centrifugation, the supernatants were transferred to a HPLC vial and analysed by LC-MS/MS (Micromass Micro triple quadrupole mass spectrometer (Water Corp., Milford, USA). The system consisted of a 5 cm x 3.2 mm Kromasil KR-100 C18 column (Hichrom, Theale, UK) and employed a mobile phase of acetonitrile and 25 mM ammonium formate pH 3. A ballistic gradient was used (time and acetonitrile concentrations = 0 min, 20%; 0.5min, 90%; 3min 90%; 3.1min, 20%; 6min, 20%) with a flow rate of 0.5 mL/min. Lorazepam and diazepam were detected by MRM monitoring of the following transitions of *m/z*, 321 to 193 and 285.3 to 154.2 respectively.

Intravenous pharmacokinetics of lorazepam

The design of the microPET study was such that two doses of lorazepam were to be administered after brain radioactivity reached a peak (~10 min) and before levels of radioactivity dropped to levels at which the signal:noise ratio became an issue (~50 min). Whilst a low dose single bolus injection of lorazepam would be sufficient to achieve sustained low plasma concentrations, a combination of a higher dose bolus injection with constant infusion would be required to rapidly achieve sustained higher plasma concentrations of lorazepam. Based on the [^{3}H]flumazenil in vivo binding data, a plasma lorazepam concentration of greater than 500 ng/mL was targeted in order to give high (>80%) occupancy. The concentration of the infusion solution required to achieve this target plasma lorazepam level was calculated using equation (1);

$$C_{SS} = R_O / Cl \quad (1)$$

where C_{SS} is the required steady state plasma concentration (ng/mL), R_O the infusion rate (ng/h) and Cl the plasma clearance of lorazepam (mL/min/kg).

The i.v. pharmacokinetics of lorazepam were investigated in male CD rats (~300g), in which a jugular vein cannula was exteriorised at the nape of the neck, under isoflurane anaesthesia. Animals were allowed to recover for a minimum of 36 h during which they were freely moving and singly housed. Lorazepam, formulated as an aqueous solution in 2% DMSO/10% hydroxypropyl-β-cyclodextrin, was administered via a bolus tail vein injection (1 mL/kg) at 0.05, 0.1 or 0.5 mg/kg, one rat per dose level and blood was serially sampled via the indwelling cannula up to 3 h post dose. Pharmacokinetic parameters were calculated from plasma-time data by model-independent methods using in-house software.

Following determination of the plasma clearance of lorazepam, a dosing regime was constructed to facilitate the desired high plasma lorazepam concentrations to achieve ~80% receptor occupancy. To examine the utility of this dosage regime, dual jugular and femoral vein cannulated male CD rats (~300g) were surgically prepared under isoflurane anaesthesia. Rats freely moving and tethered, to protect the exteriorised infusion and blood sampling cannulae, were singly housed and allowed to recover for a minimum of 36 h. Rats (n=3 per dose group) were dosed with a bolus loading dose of lorazepam (0.5 mg/kg, 1 mL/kg) and/or an infusion of lorazepam (0.2 mg/mL) administered via the femoral vein cannula, delivered at a rate of 6 mL/h/kg by a Harvard Model S infusion pump (Harvard Apparatus). Lorazepam was formulated as aqueous solutions in 2% DMSO/10% hydroxypropyl-β-cyclodextrin. Blood was serially sampled via the jugular vein cannula at time points up to 1h after the start of the infusion.

MicroPET simulation studies

To examine the potential effect of anaesthetic on both the pharmacokinetics of lorazepam and receptor occupancy measurements, a study was conducted in terminally anaesthetised male CD rats (~300g) to mimic the microPET protocol. Rats were maintained under isoflurane anaesthesia (1.5%) throughout the surgical procedure and subsequent microPET simulation. Following a small skin incision

above the right femoral triangle, the femoral artery and vein (for blood sampling and compound administration, respectively) were cannulated with polypropylene cannulae, the patency checked and the cannulae flushed with heparinised saline (50 IU/mL) prior to suturing of the skin incision.

Following a 10 min post surgical non-recovery period two doses of lorazepam were administered as follows: low dose lorazepam, 0.075 mg/kg i.v. bolus, t=10 min; high dose lorazepam, 0.5 mg/kg intravenous bolus followed by continuous infusion of 0.2 mg/mL lorazepam (6 mL/h/kg), t=21 min. Blood was sampled via the femoral artery cannula at 11, 15, 20, 22, 23, 27, 32, 42 and 52 min post surgery. To define levels of total and non specific binding, two separate groups of anaesthetised rats were dosed with vehicle (1 mL/kg, i.v., n=5) or bretazenil (5 mg/kg, 1 mL/kg i.p., 100% PEG 300, n=3), respectively, and culled 30 min post dose. All lorazepam formulations were made up as aqueous solutions in 2% DMSO/10% hydroxypropyl-β-cyclodextrin. At each time point, one rat was culled and at the 15, 20, 27, 32, 42 and 52 min times, occupancy was determined following prior i.v. administration of [^{3}H]flumazenil, as described above. Aliquots of plasma were frozen and stored at -20°C prior to subsequent analysis of drug concentrations.

MicroPET studies

[^{11}C]Flumazenil was produced from [^{11}C]iodomethane using a modified captive solvent method (Cleij et al., 2006). Radiochemical yields of 8-10 GBq and specific radioactivities of 520-600 GBq/μmol were achieved at the end of the syntheses. The [^{11}C]flumazenil was formulated in 1 ml saline containing 5% v/v ethanol with the molar amount of co-injected unlabelled flumazenil being kept constant at ~0.3 nmol by adjusting the amount of injected radioactivity, which varied between 59-90 MBq.

An overview of the design of the microPET study is presented in Figure 1. Each microPET experiment was designed to allow each animal to receive two doses of either vehicle (n=2 rats) or

lorazepam (n=5) and therefore generate two data points per animal. During this period, plasma samples were taken for subsequent analysis of lorazepam concentrations.

In brief, male CD rats (~300g) were prepared as described above for the microPET simulation studies with an additional cannula implanted into the left femoral vein for administration of the [^{11}C]flumazenil. The cannulated rats were placed in the microPET P4 scanner (Concorde Microsystems Inc., Knoxville, TN, USA) and maintained under isoflurane anaesthesia throughout the duration of the experiment. The experiment was initiated by the injection of [^{11}C]flumazenil (injected over 30 sec using a syringe pump). The scanner had a 22 x 7.8 cm FOV with a resolution of 2 mm at the center, where the brain of the rat was located.

Data for lorazepam dosed PET scans were acquired over an 80 min period (16 x 0.5 min, then 72 x 1 min frames). The list-mode PET data was plotted into 3D sinograms with dead time and randoms corrections applied. Images were reconstructed from the 3D sinogram data into 0.5x0.5x0.5mm voxels in a 180x180x151 array using a version of 3D FBP (Kinahan and Rogers, 1989) with corrections for background, normalization, sensitivity and decay.

A cortical region of interest (ROI) was defined for each subject using the threshold tool in Analyze on an image produced by summing the dynamic images over the period t=6-12 min. This ROI was then applied to the dynamic images to produce a cortical time-activity curve (TAC). To produce the mean control TAC the TAC for control #2 was scaled and shifted to produce a least squares fit with the TAC for control #1 and the TACs were then averaged.

To calculate occupancy, the TAC from a displacement study was scaled and shifted to achieve the least squares fit to the mean control TAC over the range t=4-8 min using 2nd order polynomial functions. Secondly, over the period t=60-72 min an exponential was fitted to the displacement study TAC to estimate the non-specifically bound and free signal in the cortical ROI; the high dose flumazenil injection at t=46 min was assumed to have removed the specifically bound cortical signal by t=60 min. Occupancy

was then averaged over the t=15-25 min (low dose lorazepam) and t=36-46 min (high dose lorazepam) time periods using equation (2):

$$Occupancy = \frac{100}{M}\sum_{i=1}^{M}\frac{(C_i - D_i)}{(C_i - NSF_i)} \quad (2)$$

where C_i is the mean control TAC value at time point i, D_i is the displacement study TAC value at time point i, NSF_i is the estimated non-specifically bound and free signal at time point i and M is the number of time points in the period over which occupancy is being determined.

Results

In vivo binding

Figure 2A shows that the inhibition of in vivo [^{3}H]flumazenil binding by lorazepam (i.e., lorazepam occupancy) was dose-dependent with the dose required to produce 50% occupancy (ED_{50}) being 1.7 mg/kg. Measurement of plasma lorazepam concentrations showed that plasma exposure was also dose-dependent and relatively proportional.

In order to more specifically analyse the relationship between lorazepam occupancy and plasma drug concentrations suggested by the dose-dependence of these two parameters, occupancy was plotted as a function of plasma drug concentrations for each individual animal. As can be seen from Figure 3, the relationship between lorazepam occupancy and plasma drug concentrations was a sigmoidal relationship, best-fitted by a curve with a Hill slope of 0.86 and an EC_{50} of 134 ng/mL (95% confidence intervals = 119-151 ng/mL).

Rat i.v. kinetics of lorazepam

In order to design an i.v. lorazepam dosing regime suitable for the simulated as well as actual microPET studies, it was necessary to first of all measure the pharmacokinetic parameters of lorazepam following i.v. bolus dosing (Figure 4A). These experiments show lorazepam is cleared from plasma in a relatively monophasic fashion, with little evidence of a distribution phase, the latter of which is consistent with the relatively low volume of distribution (1.1 – 1.7 L/kg; Table 1). The half-life is short (0.3-0.4 hr) as a consequence of a high rate of clearance (44-54 mL/min/kg) with the similarity of all these parameters across a 10-fold dose range (0.05 to 0.5 mg/kg) suggesting that there was no saturation of clearance mechanisms at the highest dose.

Based upon these parameters, two infusion paradigms were evaluated; the first, a 0.5 mg/kg bolus followed by a 0.2 mg/kg infusion and the second, for comparative purposes, a 0.2 mg/kg infusion alone (i.e. without the bolus loading dose). As can be clearly seen from Figure 4B, the bolus followed by infusion achieved relatively constant plasma lorazepam concentrations in the region of 400-600 ng/mL. On the other hand, whilst the infusion alone ultimately gave plasma concentrations that approached those of the bolus/infusion method (~500 ng/mL), the time taken achieve these concentrations, around 1 hr, was inappropriate for the microPET experiment.

MicroPET simulation

Since the pharmacokinetic studies described above were performed in awake animals yet the microPET experiments would be performed in anaesthetised rats, we performed a microPET simulation experiment with the purpose of measuring plasma lorazepam concentrations in anaesthetised animals. In addition, certain animals were given [^{3}H]flumazenil in order to measure the lorazepam occupancy under these conditions. Figure 5 shows that 5-10 min after administration of the low dose of lorazepam (0.075 mg/kg i.v.), plasma concentrations were in the region of 40 ng/mL, which were comparable to the plasma

concentrations achieved in conscious animals at 0.05 and 0.1 mg/kg doses (concentrations at 10 min = 20 and 45 ng/mL, respectively; Fig. 4A). The high dose (0.5 mg/kg bolus followed by 0.2 mg/kg infusion) achieved plasma concentrations (580-830 ng/mL) slightly higher than those observed in conscious animals (~500 ng/mL; Fig. 4B), presumably due to the lower liver blood flow (and hence reduced clearance) and changes in the distribution of lorazepam in anaesthetised animals (Bell et al., 1985; Hansen et al., 1991).

At time points corresponding to those to be used for quantification in the microPET study, the occupancy was measured following an i.v. injection of [^{3}H]flumazenil three min prior to killing. These data (Figure 6A) showed that under the lose-dose conditions, lorazepam gave occupancy of 33 ± 2% whereas under the high-dose conditions occupancy was 83 ± 3%. From the occupancy data, and knowing the corresponding plasma drug concentrations, occupancy could be plotted as a function of plasma drug concentrations (Figure 6B). From these data, the plasma concentration corresponding to 50% occupancy was estimated at 94 ng/mL (95% confidence intervals = 63-139 ng/mL).

microPET

The average plasma lorazepam concentrations and representative rat brain time-activity curves are shown in Figure 7. The plasma kinetics of lorazepam were very similar to those of the microPET simulation experiment with plasma concentrations after administration of the low and high doses being in the region of 30-60 ng/mL and 550 ng/mL, respectively. The time-activity curves for rat brain [^{11}C]flumazenil radioactivity (Figure 7B) shows that in a control (vehicle-treated) animal, radioactivity is rapidly cleared from the brain with a half-life in the region of 20 min., which compares with the half-life of 8 and 16 min previously reported in the mouse and rat brain, respectively (Lister et al., 1984; Atack et al., 1999). Administration of a low dose of lorazepam followed by a high dose produced sequential reductions in brain [^{11}C]flumazenil, consistent with lorazepam displacing [^{11}C]flumazenil from the

benzodiazepine site of $GABA_A$ receptors. Finally, i.v. administration of unlabelled flumazenil produced essentially a complete inhibition of [^{11}C]flumazenil binding, thereby demonstrating that [^{11}C]flumazenil has very low levels of non-specific binding. Representative images of brain [^{11}C]flumazenil in vehicle- and high dose-lorazepam treated rats (inset Figure 7B) show that in control animals the uptake of [^{11}C]flumazenil into the brain was widespread and consistent with the distribution of benzodiazepine binding sites in the brain and that lorazepam produced a qualitatively equivalent reduction in [^{11}C]flumazenil in different regions of the brain, consistent with its equivalent affinity for the different $GABA_A$ receptor subtypes.

Quantitation of the inhibition of [^{11}C]flumazenil binding under the low- and high-dose conditions showed (Figure 8A) that lorazepam produced occupancy of 23 ± 3% and 86 ± 1%, respectively, which compare well with occupancy measured in the microPET simulation study (33 ± 2% and 83 ± 3%, respectively; Fig. 6A). The plasma-occupancy relationship for the microPET data was fitted by a curve with a Hill slope of 1.13 and an EC_{50} of 96 ng/mL (95% confidence intervals = 74-124 ng/mL). These data are consistent with the EC_{50} values of 134 and 94 mg/mL in the [^{3}H]flumazenil in vivo binding and the [^{3}H]flumazenil microPET simulation studies, respectively (Table 2).

Discussion

The development of small animal PET scanners, such as the microPET, offer the potential for the in vivo imaging of tissues in a longitudinal manner (Phelps, 2000; Yang et al., 2004; Cheery and Chatiioannou, 2005). Applications for such devices include, for example, following tumour progression or the fate of grafts (Phelps, 2000; Lu et al., 2006). More specifically, within the CNS, small animal PET imaging in rodents allows pathological changes to be monitored, for instance, after lesioning (Hume et al., 1996; Strome et al., 2006), transplantation (Torres et al., 1995) or in transgenic animals (Wang et al.,

2005). In addition, small animal PET studies permit the measurement of the occupancy of drugs. This is of particular interest since the demonstration that a potential drug crosses the blood-brain barrier and binds to its target should be a key step in the process of drug discovery. Furthermore, occupancy is a parameter that can be translated across species since PET can be used in rodents, primates and man (Phelps, 2000). The purpose of the present study, therefore, was to validate occupancy measured using microPET in relation to the more established terminal method of measuring occupancy in small animals, namely the ability of a compound to occupy receptors and therefore inhibit the binding of radioligand, with radioactivity being measured ex vivo.

For these studies we chose to examine the occupancy of lorazepam at the benzodiazepine binding site of $GABA_A$ receptors since not only is there high expression of $GABA_A$ receptors within the brain but the prototypic PET ligand for these receptors, [^{11}C]flumazenil, is well-described (Maziere et al., 1984; Abadie et al., 1992). Hence, [^{11}C]flumazenil readily penetrates through the blood-brain barrier in vivo, while its major ^{11}C-metabolite, [^{11}C]Ro 15-3890, is hydrophilic and does not (Debruyne et al., 1991). Importantly, [^{11}C]flumazenil also has high and displaceable specific binding (Samson et al., 1985; Pappata et al., 1988; Abadie et al., 1990; Fryer et al., 2002), which becomes flow-independent within a few minutes after iv administration (Koeppe et al., 1991). It should be emphasized that flumazenil binds with comparable affinity to $GABA_A$ receptors containing either an α1, α2, α3 or α5 subunit (the α subunit being a key determinant of the affinity of the benzodiazepine binding site; Atack, 2005). Since flumazenil is not subtype-selective, the inhibition of [^{3}H]- or [^{11}C]flumazenil binding by a compound such as lorazepam that also is not subtype-selective represents equivalent occupancy of the α1, α2, α3 and α5 subtypes. For example, a 75% inhibition of [^{3}H]- or [^{11}C]flumazenil by lorazepam represents equivalent (75%) occupancy at each of the four subtypes.

The measurement of lorazepam occupancy using in vivo [^{3}H]flumazenil binding and [^{11}C]flumazenil microPET differ in several key respects. Thus, the former involves oral predosing of

lorazepam to awake animals and then injecting radioligand and measuring the extent by which in vivo [^{3}H]flumazenil binding, measured ex vivo, is reduced relative to a group of vehicle-treated animals; in the latter [^{11}C]flumazenil is administered first and then this binding is displaced by i.v. administration of lorazepam with the extent of this displacement being calculated using an estimate of the [^{11}C]flumazenil time-activity curve had lorazepam not been administered. Despite these many methodological differences, the plasma EC_{50} values for the [^{3}H]flumazenil in vivo binding and [^{11}C]flumazenil microPET studies were very similar, being 134 and 96 ng/mL, respectively. Moreover, a hybrid of these two methods in which the microPET dosing and anaesthetic conditions were mimicked but [^{3}H]flumazenil was used as the radioligand and radioactivity was detected ex vivo rather than in vivo using PET, also gave a similar EC_{50} value, 94 ng/mL.

The similarity of the plasma lorazepam EC_{50} values for conscious animals in the [^{3}H]flumazenil in vivo binding assay and isoflurane-anaesthetised rats in the microPET studies suggests that under the conditions used, isoflurane does not appreciably alter the binding of radiolabelled flumazenil to the benzodiazepine binding site of the $GABA_A$ receptor. This is in contrast to sevoflurane and propofol which have both been reported to enhance [^{11}C]flumazenil binding in man (Salmi et al., 2004) and isoflurane which under the conditions used (Hansen et al., 1991) increased in vivo [^{3}H]flumazenil binding, although the latter was considered to be an effect on reduced hepatic clearance (Hansen et al., 1991) rather than a direct effect on the $GABA_A$ receptor (Gyulai et al., 2001). Nevertheless, it is somewhat surprising that in the present study isoflurane does not appear to significantly alter the binding of [^{3}H]flumazenil given that $GABA_A$ receptors have a distinct recognition site for isoflurane (Mihic et al. 1997; Jenkins et al., 2001; Schofield and Harrison, 2005) and isoflurane can alter the binding of radioligands to the GABA and benzodiazepine binding sites of native $GABA_A$ receptors (Harris et al., 1993, 1994). However, at the very least these data highlight the need to consider the possible effects of

anaesthetics when considering in vivo radioligand binding performed under the anaesthetized, immobile conditions required for microPET studies.

A dose of 0.075 mg/kg i.v. produced 33% or 23% occupancy in the simulation and actual microPET studies (Figures 6 and 8), corresponding to ED_{50} values of 0.15 and 0.25 mg/kg, respectively. These data are comparable to the ED_{50} for lorazepam of 0.34 mg/kg i.v. measured in baboon using [^{123}I]iomazenil single-photon emission computed tomography (SPECT; Sybirska et al., 1993). The similarity of the ED_{50} values of lorazepam in across species is mirrored by the comparably potency of flumazenil at inhibiting the binding of [^{11}C]flumazenil in baboons and man in which the ED_{50} values were 9 and ~20 ug/kg i.v., respectively, the latter being calculated on the basis of a 1.5 mg dose producing 55% occupancy (Brouillet et al., 1991; Savic et al., 1991).

In baboons, a therapeutically relevant dose of lorazepam (0.03 mg/kg i.v.) produced negligible occupancy (<5%) of benzodiazepine binding sites as measured using [^{123}I]iomazenil SPECT (Sybirska et al., 1993). Similarly, in man 1 mg of lorazepam produced occupancy, depending on brain region, of 6-9% (Lingford-Hughes et al., 2005). This level of occupancy was achieved with a mean exposure over a 90-min period of 9100 ng.min/mL, which is equivalent to an average plasma lorazepam concentration of 101 ng/mL. The fact that in man, a plasma concentration of ~100 ng/mL produced occupancy of <10% whereas in rat it is equivalent to 50% occupancy emphasizes that whereas plasma-occupancy relationships can for some compounds be relatively comparable across species, including man, this is not a general rule and plasma occupancy relationships need to be established in man using PET as part of the clinical development programme.

In summary, we have shown that two very different methods of determining receptor occupancy, namely the inhibition of in vivo binding of radioligand by predosing of test compound followed by ex vivo detection of radioactivity or the displacement of already bound radioligand with in vivo detection using PET, gave very similar results. These two methods therefore validate each other and demonstrate

the utility of microPET as an in vivo pharmacological tool. Moreover, not only do the more traditional occupancy in vivo binding methods validate microPET but, vice versa, microPET validates "old-fashioned" occupancy measurements. These latter methodologies are much less expensive, higher throughput and do not require the infrastructure (e.g., proximity to a cyclotron, dedicated radiochemistry support etc.) associated with microPET yet the current data suggests they are an equally valid approach to measuring occupancy in preclinical species and that such data can be compared with occupancy data generated using human PET studies irrespective of the marked methodological differences.

References

Abadie P, and Baron JC (1990) In: M Diksic and RS Reba (Eds.) Neurology and Psychiatry, PET and SPECT: Principles and Application. CRS Press, pp.357-379.

Abadie P, Baron JC, Bisserbe JC, Boulenger JP, Rioux P, Travère JM, Barré L, Petit-Taboué MC, and Zarifian E (1992) Central benzodiazepine receptors in human brain: estimation of regional B_{max} and K_D values with positron emission tomography. *Eur J Pharmacol* **213:**107-115.

Atack JR, Smith AJ, Emms F, and McKernan RM (1999) Regional differences in the inhibition of mouse in vivo [^{3}H]Ro 15-1788 binding reflect selectivity for α1 versus α2 and α3 subunit-containing $GABA_A$ receptors. *Neuropsychopharmacol* **20:**255-262.

Atack JR (2005) The benzodiazepine binding site of $GABA_A$ receptors as a target for the development of novel anxiolytics. *Exp Opin Invest Drugs* **14:**601-618.

Atack JR, Wafford KA, Tye SJ, Cook SM, Sohal S, Pike A, Sur C, Melillo D, Bristow L, Bromidge F, Ragan I, Kerby J, Street L, Carling R, Castro JL, Whiting P, Dawson GR, and McKernan RM (2006) TPA023 [7-(1,1-dimethylethyl)-6-(2-ethyl-2*H*-1,2,4-triazol-3-ylmethoxy)-3-(2-fluorophenyl)-1,2,4-triazolo[4,3-*b*]pyridazine], an agonist selective for α2- and α3-containing $GABA_A$ receptors, is a non-sedating anxiolytic in rodents and primates. *J Pharmacol Expt Therap* **316:**410-422.

Bell LE, Slattery JT, and Calkins DF (1985) Effect of halothane-oxygen anesthesia on the pharmacokinetics of diazepam and its metabolites in rats. *J Pharmacol Exp Ther* **233:**94-99.

Brouillet E, Chavoix C, Bottlaender M, Khalili-Varasteh M, Hantraye P, Fournier D, Dodd RH, and Mazière M (1991) In vivo bidirectional modulatory effect of benzodiazepine receptor ligands on GABAergic transmission evaluated by positron emission tomography in non-human primates. *Brain Res* **557:**167-176.

Cheery SR, and Chatziioannou AF (2005) Small animal PET systems. In: MN Wernick and JN Aarsvold (Eds.) Emission Tomography – The Fundamentals of PET and SPECT. Elsevier, Amsterdam, pp. 213-228.

Cleij MC, Clark JC, Baron JC, and Aigbirhio FI (2006) Rapid preparation of [^{11}C]flumazenil: Captive solvent synthesis combined with purification by analytical sized columns. *J Labelled Compd Radiopharm* in press.

Debruyne D, Abadie P, Barre L, Albessard F, Moulin M, Zarifian E, and Baron JC (1991) Plasma pharmacokinetics and metabolism of the benzodiazepine antagonist [^{11}C] Ro 15-1788 (flumazenil) in baboon and human during positron emission tomography studies. *Eur J Drug Metab Pharmacokinet* **16:**141-152.

Duffy RA, Varty GB, Morgan CA, and Lachowicz JE (2002) Correlation of neurokinin (NK) 1 receptor occupancy in gerbil striatum with behavioral effects of NK1 antagonists. *J Pharmacol Exp Ther* **301:**536-542.

Fryer TD, Cleij MC, Aigbirhio FI, Beech JS, Barret O, Carpenter TA, Menon DK, Clark JC, and Baron JC (2002) Imaging benzodiazepine receptors in the rat brain using [^{11}C]flumazenil and microPET. *NeuroImage* **16 (Suppl):**S26.

Gyulai FE, Mintun MA, and Firestone LL (2001) Dose-dependent enhancement of in vivo $GABA_A$-benzodiazepine receptor binding by isoflurane. *Anesthesiology* **95:**585-593.

Hansen TD, Warner DS, Todd MM, Baker MT, and Jensen NF (1991) The influence of inhalation anethetics on in vivo and in vitro benzodiazepine receptor binding in the rat cerebral cortex. *Anesthesiology* **74:**97-104.

Harris B, Wong G, and Skolnick P (1993) Neurochemical actions of inhalational anesthetics at the $GABA_A$ receptor complex. *J Pharmacol Exp Ther* **265:**1392-1398.

Harris BD, Moody EJ, Basile AS, and Skolnick P (1994) Volatile anesthetics bidirectionally and stereospecifically modulate ligand binding to GABA receptors. *Eur J Pharmacol* **267:**269-274.

Hume SP, Lammertsma AA, Myers R, Rajeswaran S, Bloomfield PM, Ashworth S, Fricker RA, Torres EM, Watson I, and Jones T (1996) The potential of high-resolution positron emission tomography to monitor striatal dopaminergic function in rat models of disease. *J Neurosci Methods* **67:**103-112.

Jenkins A, Greenblatt EP, Faulkner HJ, Bertaccini E, Light A, Lin A, Andreasen A, Viner A, Trudell JR, and Harrison NL (2001) Evidence for a common binding cavity for three general anesthetics within the $GABA_A$ receptor. *J Neurosci* **21:**RC136(1-4).

Kinahan PE, and Rogers JG (1989) Analytic 3D image reconstruction using all detected events. *IEEE Trans Nucl Sci* **36:**964−968.

Koeppe RA, Holthoff VA, Frey KA, Kilbourn MR, and Kuhl DE (1991) Compartmental analysis of [^{11}C]flumazenil kinetics for the estimation of ligand transport rate and receptor distribution using positron emission tomography. *J Cereb Blood Flow Metab* **11:**735-744.

Li J, Fish RL, Cook SM, Tattersall FD, and Atack JR (2006) Comparison of in vivo and ex vivo [^{3}H]flumazenil binding assays to determine occupancy at the benzodiazepine binding site of rat brain $GABA_A$ receptors. *Neuropharmacology* **51:**168-172.

Lingford-Hughes A, Wilson SJ, Feeney A, Grasby PG, and Nutt DJ (2005) A proof-of-concept study using [^{11}C]flumazenil PET to demonstrate that pagoclone is a partial agonist. *Psychopharmacology* **180:**789-791.

Lister RG, Greenblatt DJ, Abernethy DR, and File SE (1984) Pharmacokinetic studies on Ro 15-1788, a benzodiazepine receptor ligand, in the rat brain. *Brain Res* **290:**183-186.

Lu Y, Dang H, Middleton B, Zhang Z, Washburn L, Stout DB, Campbell-Thompson M, Atkinson MA, Phelps M, Gambhir SS, Tian J, and Kaufman DL (2006) Noninvasive imaging of islet grafts using positron-emission tomography. *Proc Natl Acad Sci USA* **103:**11294-11299.

Maziere M, Hantraye P, Prenant C, Sastre J, and Comar D (1984) Synthesis of ethyl 8-fluoro-5,6-dihydro-5-[^{11}C]methyl-6-oxo-4H-imidazo [1,5-a] [1,4]benzodiazepine-3-carboxylate (Ro 15.1788-^{11}C): a specific radioligand for the in vivo study of central benzodiazepine receptors by positron emission tomography. *Int J Appl Radiat Isot* **35:**973–976.

Mihic SJ, Ye Q, Wick MJ, Koltchine VV, Krasowski MD, Finn SE, Mascia MP, Valenzuela CF, Hanson KK, Greenblatt EP, Harris RA, and Harrison NL (1997) Sites of alcohol and volatile anaesthetic action on $GABA_A$ and glycine receptors. *Nature* **389:**385-389.

Pappata S, Samson Y, Chavoix C, Prenant C, Mazière M, and Baron JC (1988) Regional specific binding of [^{11}C]RO 15 1788 to central type benzodiazepine receptors in human brain: quantitative evaluation by PET. *J Cereb Blood Flow Metab* **8:**304-313.

Phelps ME (2000) Positron emission tomography provides molecular imaging of biological processes. *Proc Natl Acad Sci USA* **97:**9226-9233.

Salmi E, Kaisti KK, Metsähonkala L, Oikonen V, Aalto S, Någren K, Hinkka S, Hietala J, Korpi ER, and Scheinin H (2004) Sevoflurane and propofol increase ^{11}C-flumazenil binding to gamma-aminobutyric acid$_A$ receptors in humans. *Anesth Analg* **99:**1420-1426.

Samson Y, Hantraye P, Baron JC, Soussaline F, Comar D, and Mazière M (1985) Kinetics and displacement of [^{11}C]RO 15-1788, a benzodiazepine antagonist, studied in human brain in vivo by positron tomography. *Eur J Pharmacol*, **110:**247-251.

Savic I, Widen L, and Stone-Elander S (1991) Feasibility of reversing benzodiazepine tolerance with flumazenil. *Lancet* **337:**133-137.

Schofield, C.M., and Harrison, N.L. (2005) Transmembrane residues define the action of isoflurane at the GABA$_A$ receptor alpha-3 subunit. *Brain Res* **1032:**30-35.

Strome EM, Cepeda IL, Sossi V, and Doudet DJ (2006) Evaluation of the integrity of the dopamine system in a rodent model of Parkinson's disease: small animal positron emission tomography compared to behavioral assessment and autoradiography. *Mol Imaging Biol* **8:**292-299.

Sybirska E, Seibyl JP, Bremner JD, Baldwin RM, al-Tikriti MS, Bradberry C, Malison RT, Zea-Ponce Y, Zoghbi S, During M, Goddard AW, Woods SW, Hoffer PB, Charney DS, and Innis RB (1993) [^{123}I]iomazenil SPECT imaging demonstrates significant benzodiazepine receptor reserve in human and nonhuman primate brain. *Neuropharmacology* **32:**671-80.

Tai C, Chatziioannou, A, Siegel S, Young J, Newport D, Goble RN, Nutt RE, and Cherry SR (2001) Performance evaluation of the microPET P4: a PET system dedicated to animal imaging. *Phys Med Biol* **46:**1845-1862

Takasawa M, Beech JS, Fryer TDF, Hughes JL Igase K, Jones PS, Smith R, Aigbirhio FI, Menon DK, Clark JC, and Baron JC (2006). Imaging of brain hypoxia in permanent and temporary middle

cerebral artery occlusion in the rat using (^{18})F-fluoromisonidazole and positron emission tomography: a pilot study. *J Cereb Blood Flow Metab* (in press).

Torres EM, Fricker RA, Hume SP, Myers R, Opacka-Juffry J, Ashworth S, Brooks DJ, and Dunnett SB (1995) Assessment of striatal graft viability in the rat in vivo using a small diameter PET scanner. *Neuroreport* **6:**2017-2021.

Wang J, and Maurer L (2005) Positron emission tomography: applications in drug discovery and drug development. *Curr Top Med Chem* **5:**1053-1075.

Wang X, Sarkar A, Cicchetti F, Yu M, Zhu A, Jokivarsi K, Saint-Pierre M, and Brownell AL (2005) Cerebral PET imaging and histological evidence of transglutaminase inhibitor cystamine induced neuroprotection in transgenic R6/2 mouse model of Huntington's disease. *J Neurol Sci* **231:**57-66.

Yang Y, Tai YC, Siegel S, Newport DF, Bai B, Li Q, Leahy RM, and Cherry SR (2004) Optimization and performance evaluation of the microPET II scanner for in vivo small-animal imaging. *Phys Med Biol* **49:**2527-2545.

Legends for Figures

Figure 1. Schematic representation of the design of the [^{11}C]flumazenil microPET study. At t=0, [^{11}C]flumazenil was administered and after 10 min a low dose of lorazepam was administered (0.75 mg/kg i.v.). A high dose of lorazepam (0.5 mg/kg bolus followed by a 0.2 mg/mL, 6 mL/kg/hr infusion) was then given 26 min after commencement of the study. At t=46 min unlabelled flumazenil was given and was used to define the extent of non-specific binding and free [^{11}C]flumazenil.

Figure 2. Rat brain lorazepam occupancy and plasma drug concentrations 30 min after p.o. dosing as a suspension in 0.5% methyl cellulose. A. Lorazepam occupancy, as measured using a [^{3}H]flumazenil in vivo binding assay, increases as a function of dose, with the dose of lorazepam required to occupy 50% of binding sites (ED_{50}) being 1.7 mg/kg. B. Plasma lorazepam concentrations were also proportional to the dose. Values shown are mean ± SEM (n=5-10/group).

Figure 3. The relationship between rat plasma lorazepam concentrations and occupancy as measured using [^{3}H]flumazenil in vivo binding. The plasma lorazepam concentration required to produce 50% occupancy (ED_{50}) was 134 ng/mL. Each data point represents an individual animal.

Figure 4. Kinetics of lorazepam in rat plasma. A. Kinetics following i.v. bolus doses of 0.05, 0.1 and 0.5 mg/kg to individual rats B. Plasma profile of lorazepam following a bolus loading dose (0.5 mg/kg, 1 mL/kg) of lorazepam and/or an infusion of lorazepam (0.2 mg/mL infused at a rate of 6 mL/h/kg) administered via the femoral vein cannula. Values shown are mean ± SEM (n=3/group).

Figure 5. Plasma concentrations of lorazepam dosed under simulated microPET conditions. Nine anaesthetised rats were cannulated and serial blood samples collected and plasma lorazepam concentrations were measured. Lorazepam was administered i.v. as a low dose (t=10 min, 0.075 mg/kg) and a high dose (t=21 min, 0.5 mg/kg bolus followed by 0.2 mg/mL, 6 mL/h/kg infusion). At each time point an animal was killed and occupancy was measured at the 15, 20, 27, 32, 42 and 52 min time points (denoted by arrows). Values shown are mean ± SEM (n=9 at 11 min time point, decreasing sequentially to n=1 at the 52 min time point). Arrows indicate the times at which rats were taken and occupancy measured (Figure 6).

Figure 6. Results of microPET simulation assay using [^{3}H]flumazenil. A. Mean occupancy (± SEM) during low dose (0.075 mg/kg i.v.) and high dose (0.5 mg/kg i.v. bolus followed by 0.2 mg/mL, 6 mL/h/kg infusion). Single animals were killed at the 15 and 20 min. time points (low dose lorazepam) and at the 27, 32, 42 and 52 min. time points (high dose lorazepam) and the brain removed, homogenised, filtered and washed. Membrane-bound [^{3}H]flumazenil binding was quantified by liquid scintillation counting and the extent to which lorazepam inhibited [^{3}H]flumazenil binding (i.e. occupancy) calculated. B. Occupancy plotted as a function of the concentration of lorazepam in plasma. Each data point represents an individual animal. The plasma concentration estimated to give 50% occupancy was 94 ng/mL (Hill slope = 0.87).

Figure 7. Kinetics of plasma lorazepam concentrations and brain radioactivity during the microPET study. A. Plasma concentrations (mean ± SEM, n=5) in blood obtained from the femoral artery. Open and filled arrows represent the start of the low dose (0.075 mg/kg) and high dose (0.5 mg/kg i.v. bolus followed by 0.2 mg/mL, 6 mL/h/kg infusion) lorazepam administrations, respectively. B. Representative time-activity curves for [^{11}C]flumazenil in brain of rats treated with either vehicle (2% DMSO/10% hydroxypropyl-ß-cyclodextrin) or lorazepam. Non-specific binding and free [^{11}C]flumazenil (NSF) was defined lorazepam-treated animals which then received a dose of flumazenil (0.25 mg/kg i.v.; t=46 min) which gave complete displacement of [^{11}C]flumazenil from benzodiazepine binding sites. Data for NSF prior to t=46 was derived by backwards extrapolation of an exponential function. Pseudocolour images show the decay-corrected distribution of [^{11}C]flumazenil in representative horizontal sections of the brains of single rats treated with either vehicle (Veh.) or lorazepam (Lor.) with images being acquired over 10 min periods commencing 15 or 36 min after the experiment began (periods corresponding to low- and high-dose lorazepam periods, respectively).

Figure 8. Inhibition of [^{11}C]flumazenil binding to the benzodiazepine site of rat brain $GABA_A$ receptors by lorazepam. A. Mean levels of inhibition of [^{11}C]flumazenil binding (i.e. lorazepam occupancy) following low and high doses of lorazepam. Bars show mean ± SEM (n=5) with data from individual animals also being presented. B. Occupancy plotted as a function of the concentration of lorazepam in plasma. Data was derived from five rats with occupancy being measured for each animal during the low dose (0.075 mg/kg i.v. bolus; t = 20 min) and high dose (0.5 mg/kg bolus followed by 0.2 mg/mL, 6 mL/h/kg infusion; t = 46 min) phases of the study. The plasma concentration estimated to give 50% occupancy was 96 ng/mL (Hill slope = 1.13). The curves fitted to the in vivo [^{3}H]flumazenil binding and microPET simulation data (Figs. 3 and 6B, respectively) are included for comparison.

Table 1: Pharmacokinetic parameters of lorazepam in rat plasma after i.v. bolus administration

Parameter	Lorazepam i.v. dose, mg/kg		
	0.05	0.1	0.5
$AUC_{0\text{-}3h}$ (ng.hr/mL)	15	38	175
Cl (mL/min/kg)	54	44	48
$T_{½}$ (h)	0.3	0.4	0.3
Vd (L/kg)	1.1	1.1	1.7

$AUC_{0\text{-}3h}$ = area under the curve integrated over the period of 0 to 3 hr

Cl = Clearance; $T_{½}$ = plasma half-life; Vd = volume of distribution

Table 2: Summary of plasma lorazepam concentrations required to produce 50% occupancy of rat brain $GABA_A$ receptors as measured using different methods

	Plasma lorazepam conc., ng/mL	
Assay	EC_{50}	95% confidence intervals
[^{3}H]flumazenil in vivo binding	134	119-151
[^{3}H]flumazenil microPET simulation	94	63-139
[^{11}C]flumazenil microPET	96	74-124

JPET Fast Forward. Published on December 12, 2006 as DOI: 10.1124/jpet.106.114884
This article has not been copyedited and formatted. The final version may differ from this version.

Figure 1

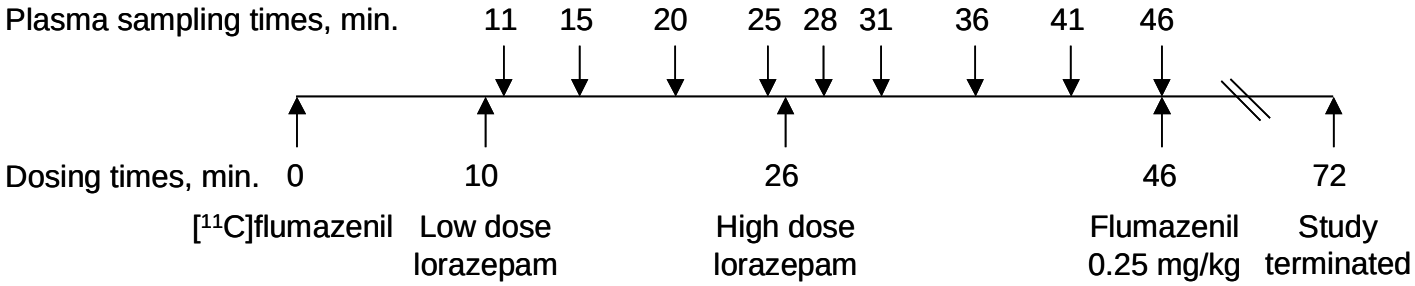

JPET Fast Forward. Published on December 12, 2006 as DOI: 10.1124/jpet.106.114884
This article has not been copyedited and formatted. The final version may differ from this version.

Figure 2

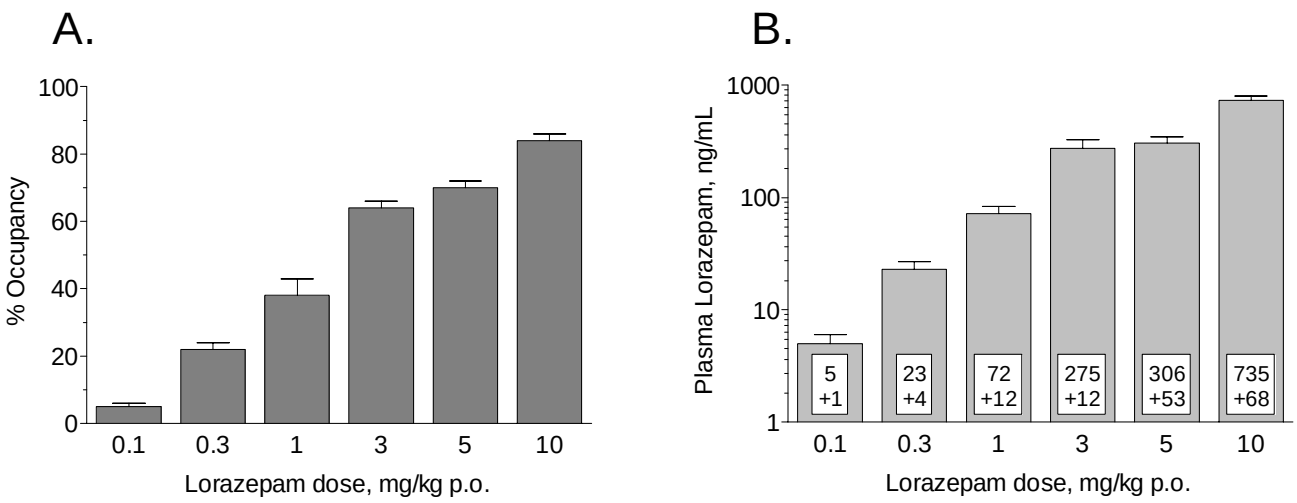

JPET Fast Forward. Published on December 12, 2006 as DOI: 10.1124/jpet.106.114884
This article has not been copyedited and formatted. The final version may differ from this version.

Figure 3

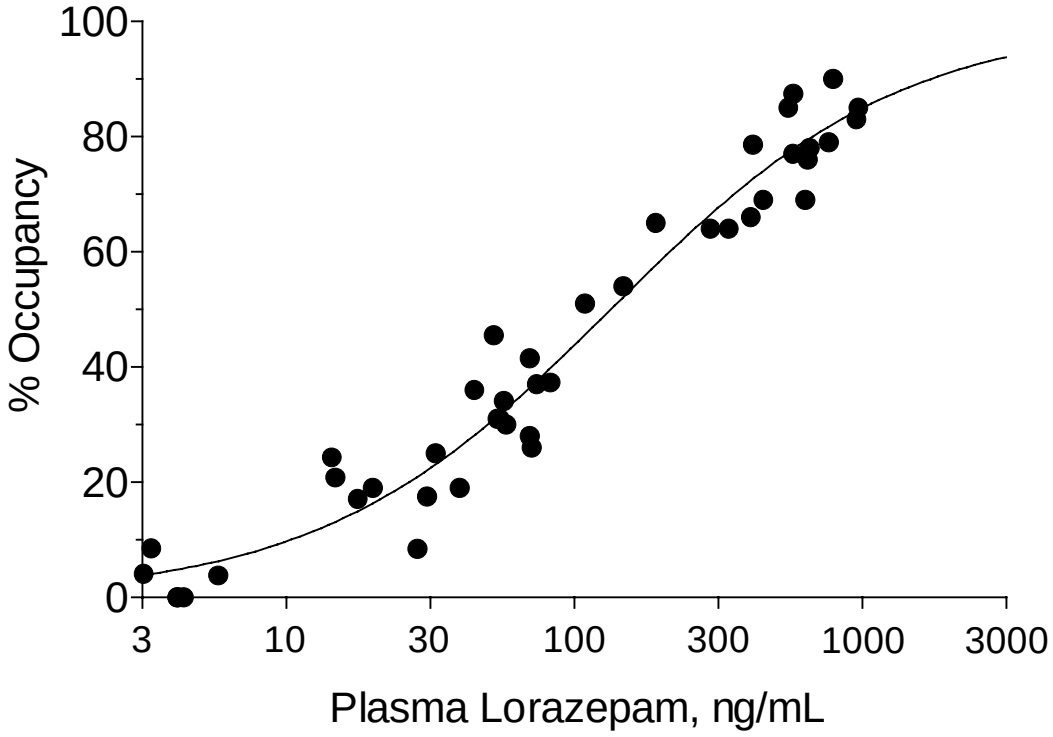

JPET Fast Forward. Published on December 12, 2006 as DOI: 10.1124/jpet.106.114884
This article has not been copyedited and formatted. The final version may differ from this version.

Figure 4

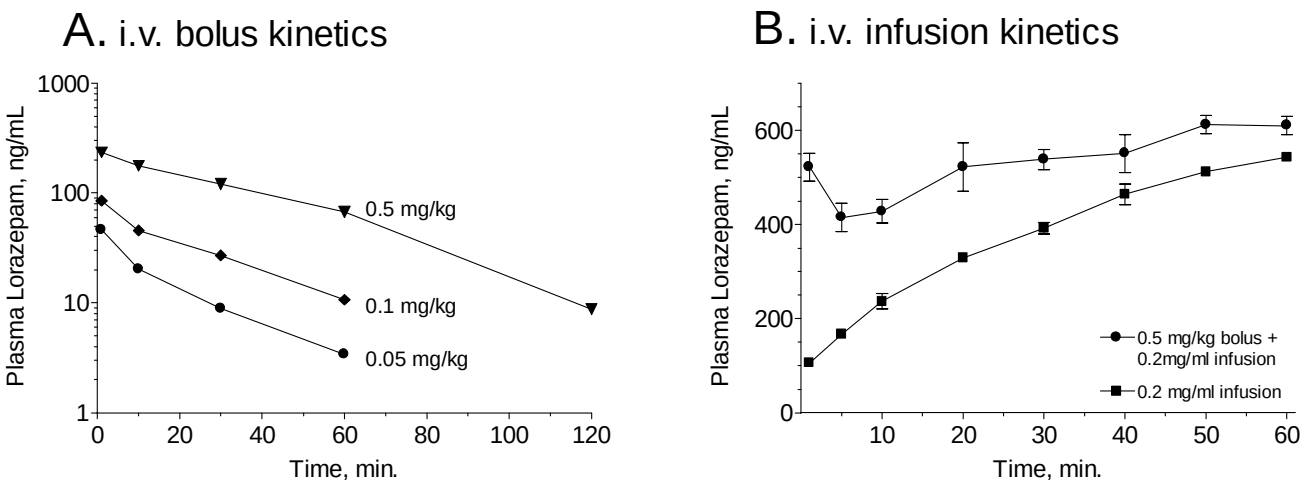

JPET Fast Forward. Published on December 12, 2006 as DOI: 10.1124/jpet.106.114884
This article has not been copyedited and formatted. The final version may differ from this version.

Figure 5

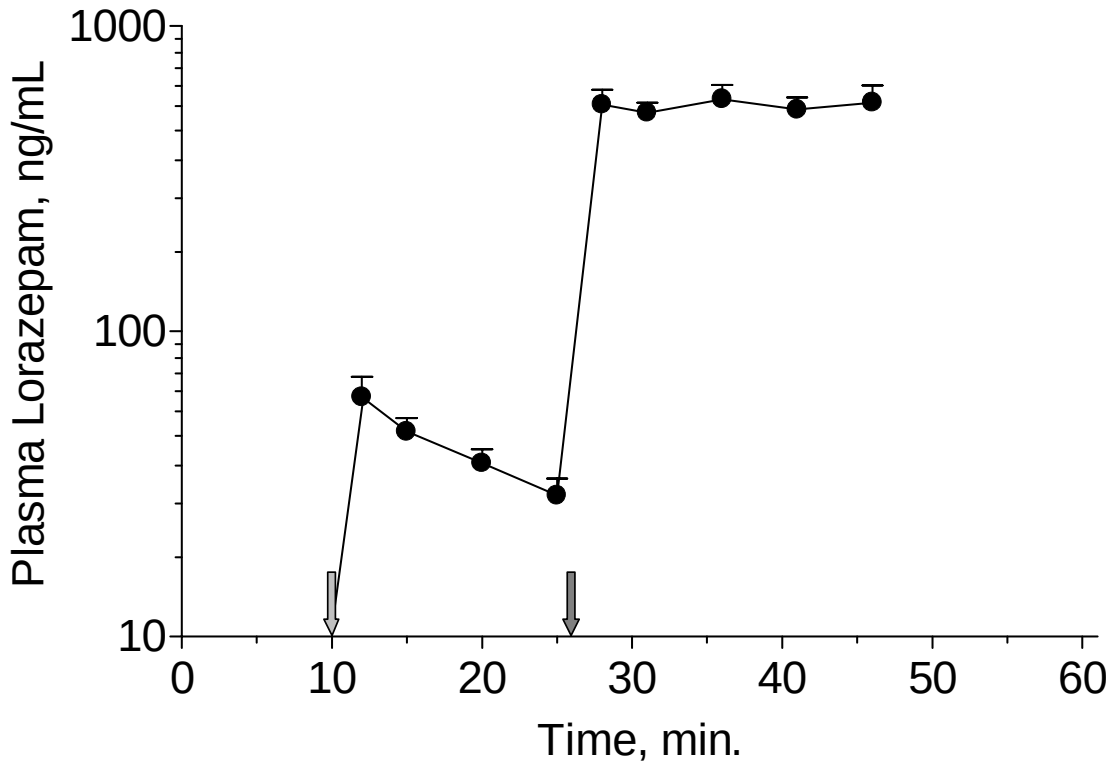

JPET Fast Forward. Published on December 12, 2006 as DOI: 10.1124/jpet.106.114884
This article has not been copyedited and formatted. The final version may differ from this version.

Figure 6

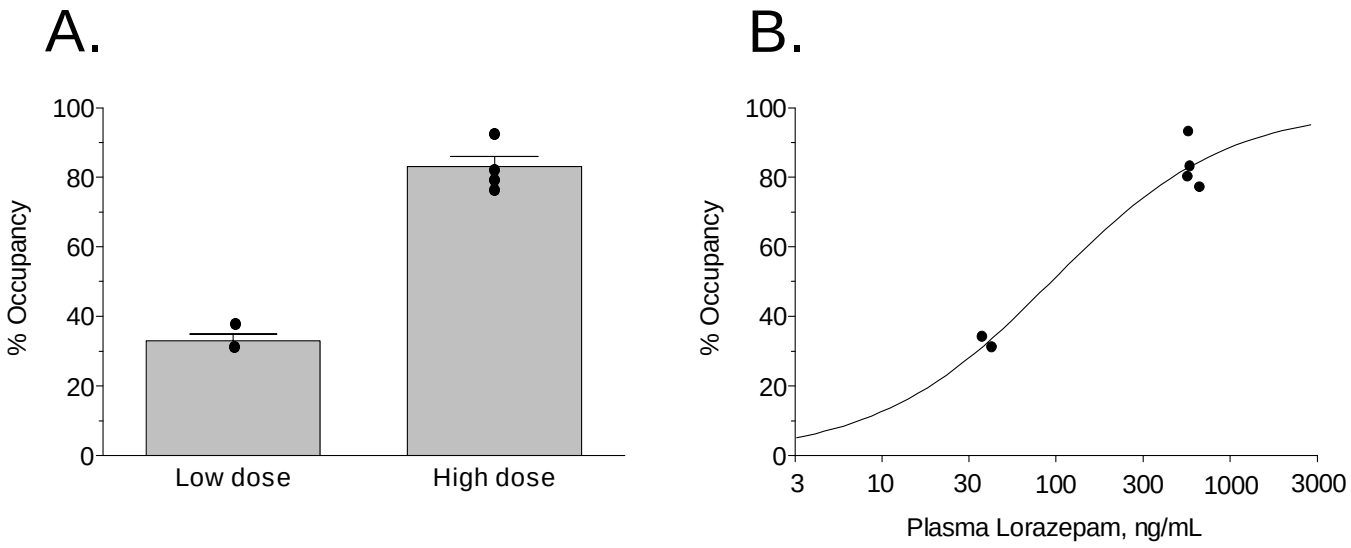

JPET Fast Forward. Published on December 12, 2006 as DOI: 10.1124/jpet.106.114884
This article has not been copyedited and formatted. The final version may differ from this version.

Figure 7

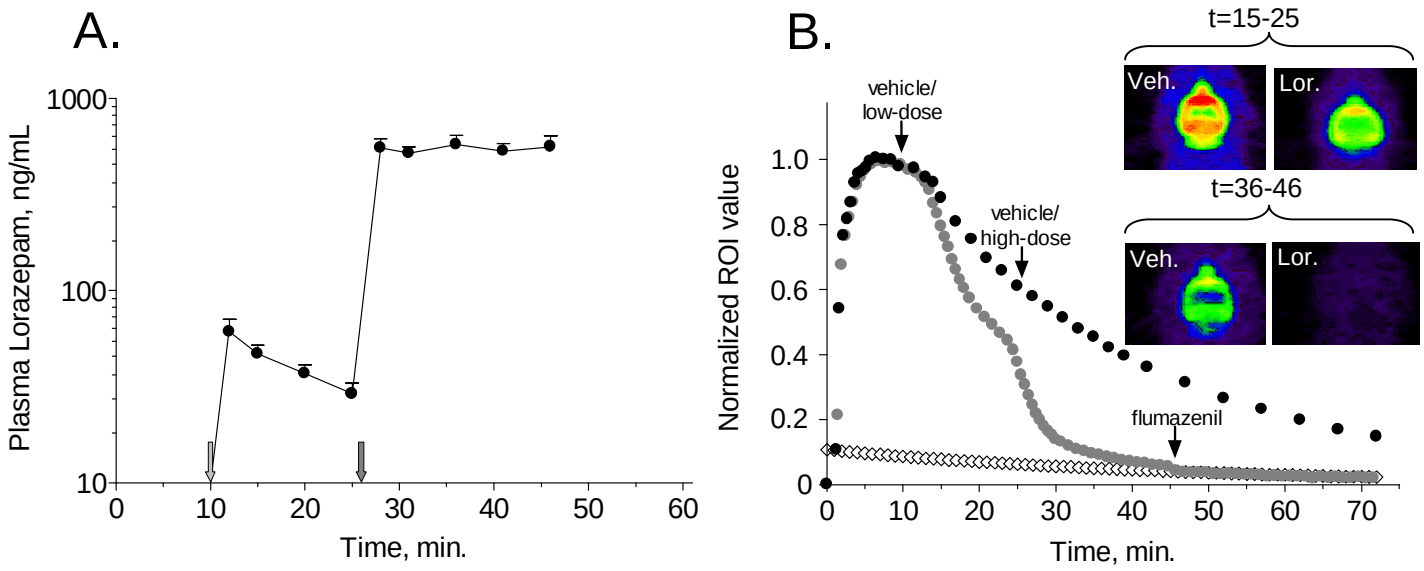

JPET Fast Forward. Published on December 12, 2006 as DOI: 10.1124/jpet.106.114884
This article has not been copyedited and formatted. The final version may differ from this version.

Figure 8